

Allyl palladium dithiocarbamates and related dithiolate complexes as precursors to palladium sulfides

Anthony Birri ^a, Benjamin Harvey ^a, Graeme Hogarth ^{a,*}, Elif Subasi ^{b,*}, Fadime Uğur ^c

^a Department of Chemistry, University College London, 20 Gordon Street, London WC1H 0AJ, UK

^b Department of Chemistry, Faculty of Science and Arts, Dokuz Eylül University, 35160 Buca, İzmir, Turkey

^c Ege University, Faculty of Science, Department of Chemistry, Bornova, 35100 İzmir, Turkey

Received 4 December 2006; received in revised form 9 February 2007; accepted 15 February 2007

Available online 21 February 2007

Abstract

Allyl-palladium dithiocarbamate complexes, $[\text{Pd}(\text{allyl})(\text{S}_2\text{CNR}_2)]$, have been prepared from the addition of dithiocarbamate salts to $[\text{Pd}(\text{allyl})(\mu\text{-Cl})_2]$ and TGA and DSC studies have been carried out in order to assess their potential as MOCVD precursors to palladium sulfides. For comparison $[(\eta^3\text{-C}_4\text{H}_7)\text{Pd}(\text{S}_2\text{PPh}_2)]$ and $[\text{Pd}(\text{S}_2\text{CNMeR})_2]$ ($\text{R} = \text{Bu}, \text{Hex}$) have also been prepared and tested as precursors. The unsymmetrical dithiocarbamate complex, $[(\eta^3\text{-C}_3\text{H}_5)\text{Pd}(\text{S}_2\text{CNMeHex})]$, which has a melting point of 65 °C was selected as the best single source precursor and thin films of predominantly $\text{Pd}_{2.8}\text{S}$ were deposited on glass slides. The crystal structures of $[(\eta^3\text{-C}_4\text{H}_7)\text{Pd}(\text{S}_2\text{CNMe}_2)]$, $[(\eta^3\text{-C}_4\text{H}_7)\text{Pd}(\text{S}_2\text{CNPr}_2)]$, $[(\eta^3\text{-C}_4\text{H}_7)\text{Pd}(\text{S}_2\text{PPh}_2)]$ and $[\text{Pd}(\text{S}_2\text{CNMeBu})_2]$ are reported. All except $[(\eta^3\text{-C}_4\text{H}_7)\text{Pd}(\text{S}_2\text{CNPr}_2)]$ show weak intermolecular $\text{S}\cdots\text{H}$ or $\text{Pd}\cdots\text{H}$ interactions.

© 2007 Elsevier B.V. All rights reserved.

Keywords: Dithiocarbamate; Palladium; Dithiolate; Allyl; MOCVD; X-ray; TGA; DSC

1. Introduction

A range of palladium sulfides are known including PdS , PdS_2 , Pd_4S and non-stoichiometric materials such as $\text{Pd}_{2.2}\text{S}$ and $\text{Pd}_{2.5}\text{S}$. PdS itself is a semi-conductor ($E_g = \sim 2 \text{ eV}$) which also finds use in a wide range of catalytic processes including hydrodesulfurization [1], hydrogenation [2] and the selective synthesis of methanol from carbon monoxide and hydrogen [3]. While PdS can easily be prepared upon addition of hydrogen sulfide to tetrachloropalladate(II), in common with other metal sulfides it can be difficult to process or engineer. Jain and co-workers have reported the formation of Pd_4S upon heating thiolate-bridged complexes, $[\text{Pd}(\mu\text{-SR})(\eta^3\text{-C}_4\text{H}_7)]_2$ ($\text{R} = \text{Bu}^t, \text{Ph}, \text{C}_6\text{F}_5$), in xylene [4]. A better method of preparing such materials is to use metal organic chemical vapour deposition

(MOCVD) from a single source precursor [5]. In this manner, thin films of PdS have been prepared by Zink and co-workers from the xanthate complex $[\text{Pd}(\text{S}_2\text{COPr}^i)_2]$, thermal decomposition at 350 °C producing polycrystalline tetragonal PdS on both glass slides and silicon wafers [6]. In 2002, O'Brien and co-workers reported the use of $[\text{Pd}(\text{S}_2\text{CNMeHex})_2]$ as a precursor to the formation of thin films of PdS at 400–500 °C [7], and also prepared trioctylphosphineoxide (TOPO) capped nanoparticles of PdS upon injecting $[\text{Pd}(\text{S}_2\text{CNMeHex})_2]$ in trioctylphosphine into TOPO at 250 °C.

In our laboratory, we have been interested in developing volatile precursors for the deposition of palladium metal and palladium chalcogenides. For the deposition of thin films of palladium sulfides, we targeted allyl palladium dithiocarbamate complexes [8,9] since such materials are easy to prepare and handle and we have previously found that allyl palladium complexes exhibit relatively high volatility while decomposing cleanly. Herein, we report a comparative study of the use of bis(dithiocarbamate) and allyl

* Corresponding authors.

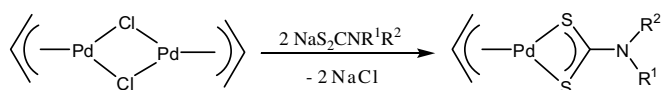
E-mail address: g.hogarth@ucl.ac.uk (G. Hogarth).

dithiocarbamate complexes as precursors to palladium sulfides.

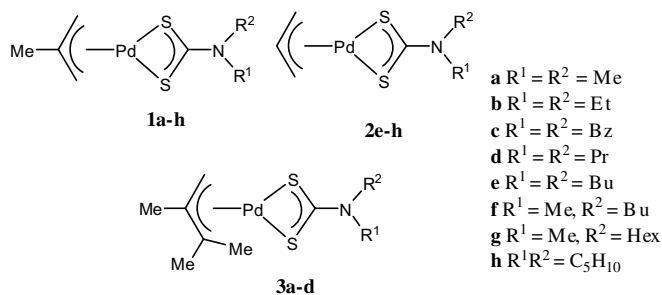
2. Results and discussion

2.1. Synthesis and characterisation

Allyl palladium dithiocarbamate complexes, $[\text{Pd}(\text{allyl})(\text{S}_2\text{CNR}_2)]$, have previously been prepared in a variety of ways [8,9]. We adopted the simple approach of Powell and Chan for their synthesis of $[(\eta^3\text{-allyl})\text{Pd}(\text{S}_2\text{CNMe}_2)]$ complexes, namely the addition of two equivalents of dithiocarbamate salts to allyl palladium chlorides $[\text{Pd}(\text{allyl})(\mu\text{-Cl})_2]$ [8]. Utilizing this simple procedure we prepared a range of complexes **1–3**.

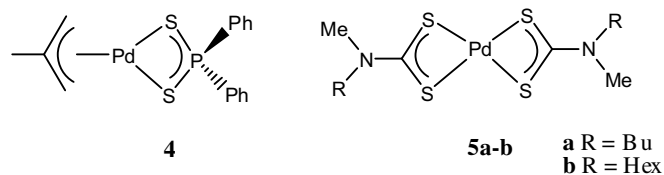


Reactions were carried out in air and work-up procedures were very simple. They proceed in good yield and are clean *provided* excess of the dithiocarbamate salts are not added. If care is not taken in this regard a secondary process occurs in which the allyl group is displaced by a dithiocarbamate to give the bis(dithiocarbamate) complexes. The dithiocarbamate salts are generated in methanol and then added to ethereal solutions of the allyl palladium chlorides. We also attempted to add aqueous solutions of dithiocarbamate salts to $[\text{Pd}(\text{allyl})(\mu\text{-Cl})_2]$ in ether but this resulted only in the formation of oily products which were not well-characterized. This is probably due to the immiscibility of water and ether resulting in poor control over the reaction stoichiometry. Reactions were generally carried out on a small scale (ca. 200 mg) and an attempt to prepare $[(\eta^3\text{-C}_4\text{H}_7)\text{Pd}(\text{S}_2\text{CNMeHex})]$ (**1g**) on a multi-gram scale gave a disappointing result with the formation of a mixture of this and the bis(dithiocarbamate) complex $[\text{Pd}(\text{S}_2\text{CNMeHex})_2]$ (**5b**). In separate work we have shown that bis(dithiocarbamate) complexes result from the addition of further dithiocarbamate salt to the allyl complexes and on a larger scale this second process becomes competitive. This problem can probably be overcome by the slow addition of the dithiocarbamate salt solution, although we did not attempt this.



Most complexes were isolated as dry solids, varying in appearance from yellow to red-brown, although a number were oily. The 1,1,2-trimethyl allyl complexes **3a–3d** were all crystalline solids, however, they were considerably less volatile than the parent or 2-methyl allyl complexes and hence not pursued further. The non-substituted allyl complexes **2e–2g** were also somewhat less volatile than those with a single methyl group on the backbone. An attempt to purify $[(\eta^3\text{-C}_4\text{H}_7)\text{Pd}(\text{S}_2\text{CNMe}_2)]$ (**1a**) by sublimation was disappointing. At 130 °C at 1 Torr it sublimed very slowly and on raising the temperature to 200–230 °C a yellow solid was deposited on the probe which was found to be $[\text{Pd}(\text{S}_2\text{CNMe}_2)_2]$. Thermal gravimetric analysis (TGA) and differential scanning calorimetry (DSC) (see later) showed loss of allyl at around 130 °C, suggesting **1a** has only limited thermal stability.

Characterization of complexes was generally straightforward. All showed absorptions in the IR spectra associated with the dithiocarbamate and allyl groups, while in the ^1H NMR spectra individual protons were generally clearly resolved. For example, $[(\eta^3\text{-C}_3\text{H}_5)\text{Pd}(\text{S}_2\text{CNMeHex})]$ (**2g**) shows a triplet of triplets at δ 5.11 for the central allyl proton, two closely spaced doublets at δ 3.98–3.97 associated with the inequivalent *syn* protons and a doublet at δ 2.71 assigned to the *anti* protons. The nitrogen-bound methyl group of the dithiocarbamate appears as a singlet at δ 3.28, the adjacent nitrogen-bound methylene group appearing at δ 3.74. Positive ion fast atom bombardment (FAB) mass spectra were generally quite distinctive. While most showed molecular ions, these were normally weak and more abundant heavier ions attributed to $[\text{Pd}_2(\text{allyl})_2(\text{dithiocarbamate})]$ and $[\text{Pd}_2(\text{allyl})(\text{dithiocarbamate})_2]$ species were observed, suggesting that loss of either the allyl and/or dithiocarbamate ligands is facile in the gas phase.



Comparison with the allyl dithiocarbamate complexes, the dithiophosphate complex $[(\eta^3\text{-C}_4\text{H}_7)\text{Pd}(\text{S}_2\text{PPh}_2)]$ (**4**) and two bis(dithiocarbamate) complexes, $[\text{Pd}(\text{S}_2\text{CNMeR})_2]$ (**5a–5b**) were also prepared. Dithiophosphate **4** was formed in essentially quantitative yield upon addition of two equivalents of NaS_2PPh_2 to $[(\eta^3\text{-C}_4\text{H}_7)\text{Pd}(\mu\text{-Cl})_2]$, while the dithiocarbamate complexes resulted from addition of two equivalents of in situ generated dithiocarbamate salts with $\text{Na}_2[\text{PdCl}_4]$ in methanol. The hexyl complex **5b** has previously been reported by O'Brien and co-workers. Their preparation was carried out in dioxane and a brown solid resulted. From methanol, both **5a–5b** are orange-yellow solids which become paler upon

sublimation. Characterization of all three was generally straightforward with evidence of fluxionality seen by ^1H NMR spectroscopy. For $[(\eta^3\text{-C}_4\text{H}_7)\text{Pd}(\text{S}_2\text{PPh}_2)]$ (**4**), while resonances associated with the allyl ligand were sharp at room temperature, all signals in the aromatic region were broadened significantly. Upon warming to 50°C these sharpened to give two multiplets centred at δ 7.86 and 7.46. The low-field signal is a doublet of doublets (J 13.7, 6.3) and is attributed to the *ortho*-protons. We attribute these changes to the rotation of the allyl ligand which renders the two phenyl groups equivalent. Room temperature ^1H NMR spectra of both **5a–b** are deceptively simple. For **5b** resonances are generally broad and smaller broad humps are seen around the major signals. Upon warming to 50°C the latter disappear and the major resonances broaden further. We associate these changes with the restricted rotation about the backbone carbon–nitrogen bonds which have some double bond character [10]. The asymmetric nature of the dithiocarbamates leads to the possibility of rotational isomers. This has previously been studied for unsymmetrical palladium(II) bis(dithiocarbamate) complexes generated from primary amines by HPLC. For $[\text{Pd}(\text{S}_2\text{CNHCH}_2\text{CH}_2\text{Ph})_2]$, a barrier to rotation of $83 \pm 5 \text{ kJ mol}^{-1}$ was measured [11]. Both **5a–5b** sublimed at 180°C at 1 Torr to give yellow solids, the ^1H NMR spectra revealing that the molecules had sublimed intact.

2.2. Structural studies

In order to fully elucidate the structures of all three types of complex and to determine if there were any intermolecular interactions which may affect the volatility of the complexes, the crystal structures of $[(\eta^3\text{-C}_4\text{H}_7)\text{Pd}(\text{S}_2\text{CNMe}_2)]$ (**1a**), $[(\eta^3\text{-C}_4\text{H}_7)\text{Pd}(\text{S}_2\text{CNPr}_2)]$ (**1d**), $[(\eta^3\text{-C}_4\text{H}_7)\text{Pd}(\text{S}_2\text{PPh}_2)]$ (**4**) and $[\text{Pd}(\text{S}_2\text{CNMeBu})_2]$ (**5a**) were carried out, the results of which are displayed in Figs. 1–4 and their captions. As expected, all contain a square-planar palladium(II) centre. In the allyl complexes this is defined by the two sulfurs of the dithiocarbamate and the outer carbons of the allyl ligand, while in **5a** it is defined by the four sulfurs. In all, the dithiolate and allyl ligands bind approximately symmetrically and geometric parameters are in line with those for related complexes. Intermolecular interactions are observed in **4** and **5a**, long range $\text{Pd}\cdots\text{H}$ interactions occurring in both (Figs. 3b and 4b). The bis(dithiocarbamate) complex **5a** adopts the *transoid* configuration and metric parameters are similar to other crystallographically characterized members of this series [12,13].

2.3. Thermal gravimetric analysis (TGA) and differential scanning calorimetry (DSC) of potential precursors

In order to assess the suitability of palladium dithiolate complexes prepared above for use as single source precursors to palladium sulfides, TGA and DSC were recorded

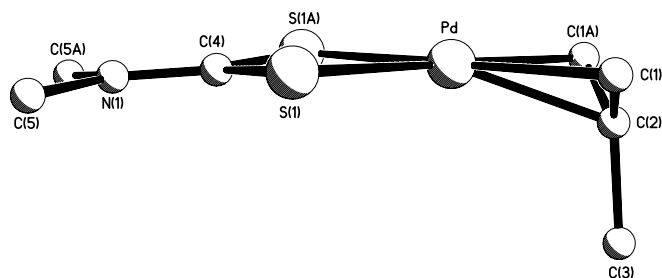


Fig. 1. Molecular structure of $[(\eta^3\text{-C}_4\text{H}_7)\text{Pd}(\text{S}_2\text{CNMe}_2)]$ (**1a**) with selected bond lengths (\AA) and angles ($^\circ$): Pd–S(1) 2.3653(13), Pd–C(1) 2.154(4), Pd–C(2) 2.122(6), S(1)–Pd–S(1A) 75.10(6), S(1)–C(4)–S(1A) 111.0(3), C(1)–Pd–C(1A) 67.5(3).

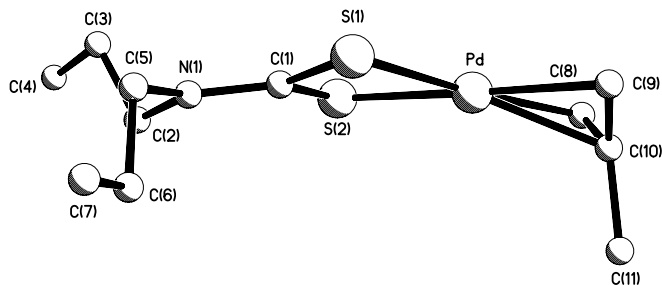


Fig. 2. Molecular structure of $[(\eta^3\text{-C}_4\text{H}_7)\text{Pd}(\text{S}_2\text{CNPr}_2)]$ (**1d**) with selected bond lengths (\AA) and angles ($^\circ$): Pd–S(1) 2.3622(12), Pd–S(2) 2.3787(13), Pd–C(8) 2.158(4), Pd–C(9) 2.146(4), Pd–C(10) 2.138(4), S(1)–Pd–S(2) 75.23(4), S(1)–C(1)–S(2) 113.7(2), C(8)–Pd–C(9) 67.3(2).

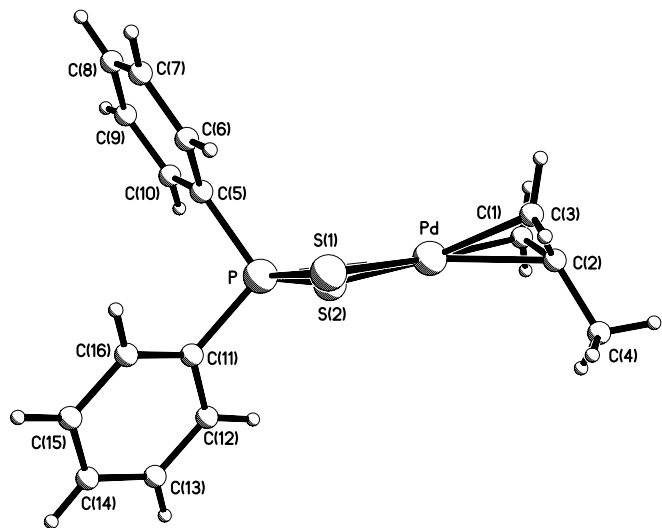


Fig. 3a. Molecular structure of $[(\eta^3\text{-C}_4\text{H}_7)\text{Pd}(\text{S}_2\text{PPh}_2)]$ (**4**) with selected bond lengths (\AA) and angles ($^\circ$): Pd–S(1) 2.410(2), Pd–S(2) 2.420(2), Pd–C(1) 2.137(7), Pd–C(2) 2.159(7), Pd–C(3) 2.130(7), Pd–P 2.961(2), S(1)–Pd–S(2) 84.56(7), S(1)–P–S(2) 107.30(11), C(1)–Pd–C(3) 68.0(3).

for a selection, the results of which are summarized in Tables 1 and 2. All experiments were carried out under a nitrogen atmosphere, heating between 20 and 500°C at a rate of $10^\circ\text{C min}^{-1}$. From TGA measurements (Table 1) the allyl dithiocarbamate complexes (Fig. 5) all showed two distinct mass losses. The first is consistent with loss

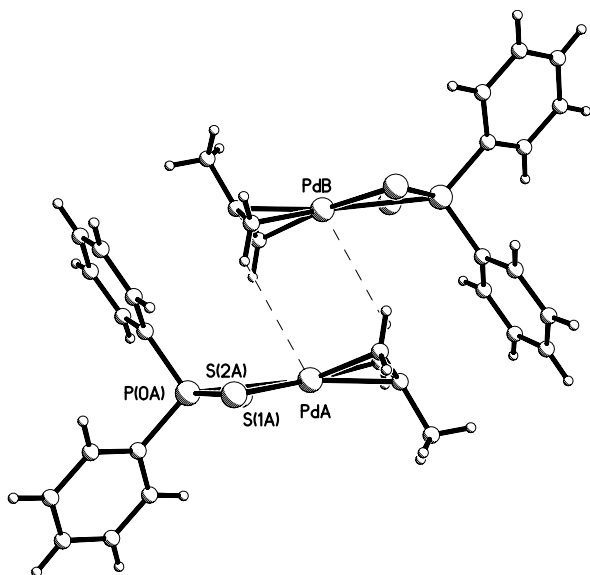


Fig. 3b. Molecular structure of $[(\eta^3\text{-C}_4\text{H}_7)\text{Pd}(\text{S}_2\text{PPh}_2)]$ (**4**) showing intermolecular interactions; $\text{Pd}\cdots\text{H}(1\text{A})$ 3.267 Å.

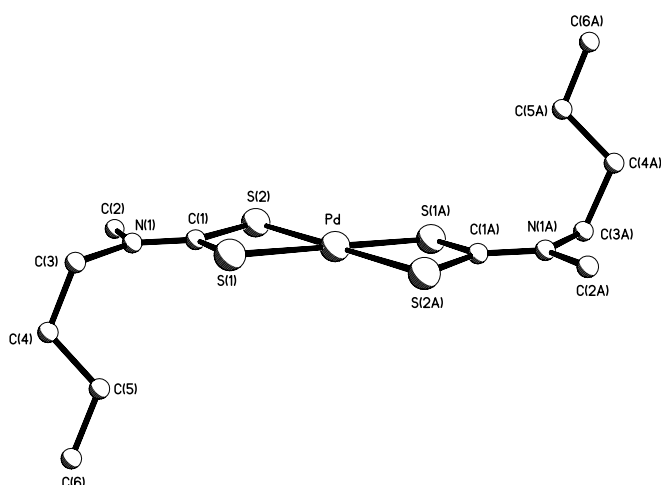


Fig. 4a. Molecular structure of $[\text{Pd}(\text{S}_2\text{CNMeBu})_2]$ (**5a**) with selected bond lengths (Å) and angles (°): $\text{Pd}\text{-S}(1)$ 2.328(2), $\text{Pd}\text{-S}(2)$ 2.333(2), $\text{S}(1)\text{-Pd}\text{-S}(2)$ 75.36(5).

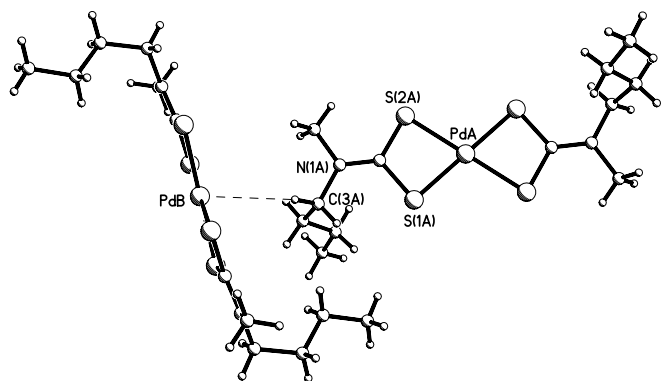


Fig. 4b. Molecular structure of $[\text{Pd}(\text{S}_2\text{CNMeBu})_2]$ (**5a**) showing intermolecular interactions; $\text{Pd}\cdots\text{H}(3\text{A})$ 3.131 Å.

of the allyl group, the lability of which was suggested from their mass spectra. DSC data (Table 2) show that this change which occurs between 128 and 166 °C is exothermic. For three of the complexes this occurs after melting, as indicated by a prior endothermic change, while for $[(\eta^3\text{-C}_3\text{H}_5)\text{Pd}(\text{S}_2\text{CNC}_5\text{H}_{10})]$ (**2h**) the loss occurs in the solid state. A second mass loss occurs between 320 and 350 °C for all four complexes and at 350 °C a mass consistent with the formation of PdS ($M = 138$) is observed. Continued heating to 500 °C gives a further gradual mass loss generally leaving materials with mass intermediate between PdS and palladium metal ($M = 106$). The exception to this is $[(\eta^3\text{-C}_4\text{H}_7)\text{Pd}(\text{S}_2\text{CNPr}_2)]$ (**1d**) which has a mass of 104 at 500 °C suggesting complete formation of palladium metal.

The allyl palladium dithiophosphinate complex, $[(\eta^3\text{-C}_4\text{H}_7)\text{Pd}(\text{S}_2\text{PPh}_2)]$ (**4**), melts at 141 °C. This then shows a slight exothermic change at 192 °C accompanied by a mass loss of 8.1%, which may be attributed to loss of the allyl group. Between 327 and 410 °C there is a further 29% mass loss, while at 500 °C the compound still has 41% of its original mass. The latter is consistent with the formation of PdS₂ ($M = 168$). The bis(dithiocarbamate) complexes, $[\text{Pd}(\text{S}_2\text{CNMeR})_2]$ (**5a–5b**), melt at 147 and 84 °C, respectively. These are low when compared to the melting point of $[\text{Pd}(\text{S}_2\text{CNET}_2)_2]$ at 243 °C, although extension of the alkyl chains such as in $[\text{Pd}(\text{S}_2\text{CNBu}_2)_2]$ reduces this to 109 °C [13]. Up to 300 °C both **5a–b** show a steady mass loss of ca. 10%, while around 380–400 °C both decompose in a single step to materials with masses consistent with the formation of palladium sulfide. Franchini and co-workers have previously shown by TGA that decomposition of $[\text{Pd}(\text{S}_2\text{CNC}_5\text{H}_{10})_2]$ occurs sequentially to give palladium sulfides, palladium metal and finally palladium oxide [14]. Their analysis was performed in air, which may account for the differences observed. O'Brien and co-workers have previously shown that **5b** decomposes to give PdS [7].

2.4. Thin film growth and characterization

In light of the TGA and DSC results discussed above we chose $[(\eta^3\text{-C}_3\text{H}_5)\text{Pd}(\text{S}_2\text{CNMeHex})]$ (**2g**) as a potential single-source precursor to palladium sulfides. This was based on its ease of formation and isolation, high level of purity, low melting point (65 °C) and smooth decomposition in two steps to leave a material with a mass equivalent to PdS at 350 °C. Approximately 200 mg of **2g** was placed in the end of a glass tube filled with overlapping glass slides and evacuated to 10^{-2} Torr. The complex was then heated to above its melting point while the centre of the tube was heated in a furnace at 350 °C. Heating was continued for 1 h resulting in the production of a thin film on two of the glass slides. The films were silver in appearance and highly reflective and were not removed from the glass by adhesive tape. The transmission and reflectance of the film was probed using UV–Vis light. The film had low transmission but was highly reflective across the whole spectrum and no maxima could be found. Energy dispersive X-ray

Table 1
Summary of TGA data

Complex	MW	First weight loss (%) (temperature range)	Second weight loss (%) (temperature range)	wt% residue (350 °C) (MW)	wt% residue (500 °C) (MW)
$[(\eta^3\text{-C}_4\text{H}_7)\text{Pd}(\text{S}_2\text{CNCPr}_2)]$ (1d)	337	19 (112–204)	37 (255–391)	38 (128)	31 (104)
$[(\eta^3\text{-C}_4\text{H}_7)\text{Pd}(\text{S}_2\text{CNC}_3\text{H}_{10})]$ (1h)	321	13 (110–175)	27 (249–318)	44 (141)	39 (125)
$[(\eta^3\text{-C}_3\text{H}_5)\text{Pd}(\text{S}_2\text{CNMeHex})]$ (2g)	337	11 (102–167)	33 (225–336)	43 (145)	39 (131)
$[(\eta^3\text{-C}_3\text{H}_5)\text{Pd}(\text{S}_2\text{CNC}_3\text{H}_{10})]$ (2h)	307	10 (102–156)	31 (256–324)	44 (135)	37 (114)
$[(\eta^3\text{-C}_4\text{H}_7)\text{Pd}(\text{S}_2\text{PPh}_2)]$ (4)	410	8 (171–219)	29 (328–410)	66 (271)	41 (168)
$[\text{Pd}(\text{S}_2\text{CNMeBu})_2]$ (5a)	430	7 (51–281)	70 (286–427)	70 (301)	20 (86)
$[\text{Pd}(\text{S}_2\text{CNMeHex})_2]$ (5b)	486	10 (56–304)	68 (309–413)	78 (379)	18 (87)

Table 2
Summary of DSC data

Complex	T_m (°C) ^a	Other peaks (°C)		
$[(\eta^3\text{-C}_4\text{H}_7)\text{Pd}(\text{S}_2\text{CNCPr}_2)]$ (1d)	41	166 ^b		
$[(\eta^3\text{-C}_4\text{H}_7)\text{Pd}(\text{S}_2\text{CNC}_3\text{H}_{10})]$ (1h)	92	137 ^b	324 ^a	329 ^b
$[(\eta^3\text{-C}_3\text{H}_5)\text{Pd}(\text{S}_2\text{CNMeHex})]$ (2g)	65	128 ^b	321 ^a	337 ^b
$[(\eta^3\text{-C}_3\text{H}_5)\text{Pd}(\text{S}_2\text{CNC}_3\text{H}_{10})]$ (2h)	–	135 ^b	321 ^a	
$[(\eta^3\text{-C}_4\text{H}_7)\text{Pd}(\text{S}_2\text{PPh}_2)]$ (4)	141	192 ^b	381 ^a	
$[\text{Pd}(\text{S}_2\text{CNMeBu})_2]$ (5a)	147	374 ^a		
$[\text{Pd}(\text{S}_2\text{CNMeHex})_2]$ (5b)	84	402 ^a		

^a Endothermic.

^b Exothermic.

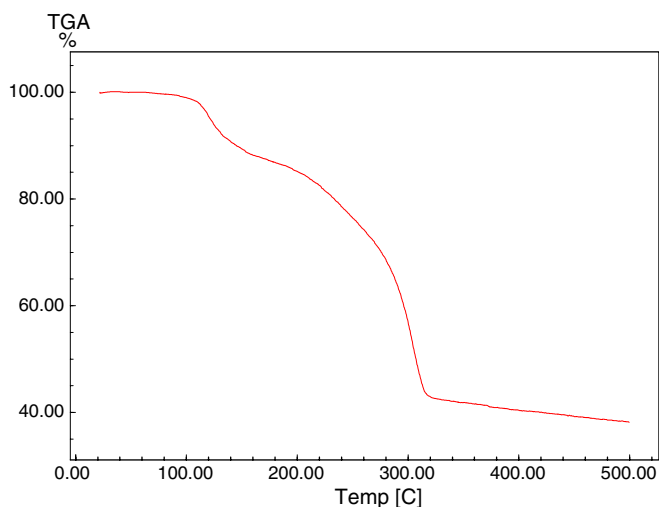


Fig. 5. TGA trace for $[(\eta^3\text{-C}_3\text{H}_5)\text{Pd}(\text{S}_2\text{CNMeHex})]$ (**2g**).

spectrometry (EDAX) of the film showed the presence of both palladium (5.85%) and sulfur (3.00% atomic composition). A scanning electron micrograph of the palladium sulfide film showed the deposited material was crystalline with an irregular surface and rough edges. A powder X-ray pattern of the film was recorded and matched against palladium sulfide materials held in the database including Pd_4S , Pd_3S , $\text{Pd}_{2.8}\text{S}$, PdS , PdS_2 . A poor match to PdS was seen, but the spectrum matched reasonably well with $\text{Pd}_{2.8}\text{S}$, Pd_3S and $\text{Pd}_{1.7}\text{S}_6$. The best match was with the phase $\text{Pd}_{2.8}\text{S}$ prepared by Grønvold and Røst upon quenching samples of Pd_3S that had been heated to 500 °C [15]. We believe that the film is a mixture containing

primarily $\text{Pd}_{2.8}\text{S}$ but also amounts of Pd_3S , Pd_4S , $\text{Pd}_{2.2}\text{S}$ and $\text{Pd}_{2.5}\text{S}$.

O'Brien and co-workers [7] and Zink and co-workers [6] have previously used homoleptic palladium dithiocarbamate and xanthate complexes, respectively, to prepare thin films of the tetragonal phase of PdS . Our results are clearly different to these. Grønvold and Røst have found that the stoichiometry of palladium sulfide phases is highly temperature dependent [15]. This may account for the difference between our results and those of O'Brien where formation of tetragonal PdS from **5b** was carried out at 500 °C. Interestingly, deposition of Pd_4S from dimeric allyl palladium dithiolate complexes is reported to occur at 200 °C. The ratio of palladium:sulfur in the nature of the materials generated and the 2:1 ratio in $[(\eta^3\text{-C}_3\text{H}_5)\text{Pd}(\text{S}_2\text{CNMeHex})]$ (**2g**) as compared to 4:1 in $[\text{Pd}(\text{dithiolate})_2]$ and 1:1 in $[(\text{allyl})\text{Pd}(\mu\text{-SR})_2]$ may play an important role in determining the nature of the films formed.

3. Conclusions

We have shown that, provided experimental conditions are carefully controlled, allyl palladium dithiocarbamate complexes can be easily prepared in high yields. With suitable substituents they have relatively low melting points, being somewhat lower than the analogous bis(dithiocarbamate) complexes. For example the melting points of $[\text{Pd}(\text{S}_2\text{CNMeHex})_2]$ (**5b**) and $[(\eta^3\text{-C}_3\text{H}_5)\text{Pd}(\text{S}_2\text{CNMeHex})]$ (**2g**) are 84 and 65 °C, respectively. Further, the allyl dithiocarbamate complexes readily lose the allyl group upon heating leading to the formation of a putative "Pd(dithiocarbamate)" fragment with a palladium:sulfur ratio of 1:2. This is different to the ratios found in previously employed precursors to palladium sulfide thin films and appears to lead to the formation of films with stoichiometries different to those from other single source precursors. We are currently investigating their utility in this regard in greater detail and will report on this in due course.

4. Experimental

Unless otherwise stated, reactions were carried out in air in non-dried solvents. Allyl palladium chlorides were prepared following the literature procedures [16] and

$\text{NaS}_2\text{CNMe}_2 \cdot 3\text{H}_2\text{O}$, $\text{NaS}_2\text{CNEt}_2 \cdot 3\text{H}_2\text{O}$ and NaS_2PPh_2 were purchased from Aldrich and used as received. IR spectra were measured as KBr discs using a Perkin–Elmer 1600 Fourier Transform Spectrophotometer. Positive-ion FAB mass spectra were recorded on a JEOL SX102 mass spectrometer operated at an accelerating voltage of 10 kV. Samples were desorbed from a nitrobenzyl alcohol matrix using 3 keV xenon atoms. Elemental analyses were performed on a Carlo Erba Strummentaione Model 1106 and ^1H and ^{31}P NMR were recorded on a Bruker FX400 spectrometer.

4.1. Synthesis of $[(\eta^3\text{-allyl})\text{Pd}(\text{S}_2\text{CNR}^1\text{R}^2)]$ (**1–3**)

All complexes were prepared by the same general method given below except for $\text{R}^1 = \text{R}^2 = \text{Me}$, Et where the sodium dithiocarbamate salts were commercially available and they were simply dissolved in methanol prior to the reaction. *N*-Methylbutylamine (74 mg, 0.85 mmol) was added to a methanol solution (10 cm³) of NaOH (34 mg, 0.84 mmol). To this CS₂ (65 mg, 0.84 mmol) was added dropwise and the solution stirred at room temperature for 30 min. A solution of $[(\eta^3\text{-C}_4\text{H}_7)\text{Pd}(\mu\text{-Cl})_2]$ (0.16 g, 0.40 mmol) in diethyl ether (40 cm³) was added and stirring was continued for a further 1 h. Removal of volatiles under reduced pressure gave a brown solid which was dissolved in dichloromethane (ca. 20 cm³), washed with water (3 × 10 cm³) and dried over MgSO₄. Removal of volatiles gave $[(\eta^3\text{-C}_4\text{H}_7)\text{Pd}(\text{S}_2\text{CNMeBu})]$ (0.201 g, 76%) as a red oil.

$[(\eta^3\text{-C}_4\text{H}_7)\text{Pd}(\text{S}_2\text{CNMe}_2)]$ (**1a**): yellow solid (78%); IR (KBr) 1525vs (CN), 1450m, 1375s, 1350m, 971s (CS); ^1H NMR (CDCl₃) δ 3.79 (s, 2H, H_{syn}), 3.33 (s, 6H, NMe), 2.62 (s, 2H, H_{anti}), 1.91 (s, 3H, Me); FAB MS (+ve) *m/z* 161 (13%), 194 (18%), 228 (42%), 281 (25%), 444 (50%), 509 (12%). Anal. Calc. for Pd₁S₂N₁C₇H₁₃: C, 29.89; H, 4.63; N, 4.98. Found: C, 29.62; H, 4.01; N, 4.70%. Single crystals suitable for diffraction studies were grown upon slow evaporation of a saturated diethyl ether solution.

$[(\eta^3\text{-C}_4\text{H}_7)\text{Pd}(\text{S}_2\text{CNEt}_2)]$ (**1b**): red solid (76%); IR (KBr) 1525vs (CN), 1440m, 1375s, 1350m, 988s (CS); ^1H NMR (CDCl₃) δ 3.71 (m, 6H, H_{syn} + NCH₂), 2.57 (s, 2H, H_{anti}), 1.87 (s, 3H, Me), 1.22 (t, *J* 7.1, 6H, Me); FAB MS (+ve) *m/z* 161 (32%), 222 (42%), 254 (100%), 311 (30%), 472 (72%), 565 (64%). Anal. Calc. for Pd₁S₂N₁C₉H₁₇.0.5CH₂Cl₂: C, 32.40; H, 5.12; N, 3.99. Found: C, 32.09; H, 5.25; N, 4.26%.

$[(\eta^3\text{-C}_4\text{H}_7)\text{Pd}(\text{S}_2\text{CNBz}_2)]$ (**1c**): yellow solid (65%); IR (KBr) 1500vs (CN), 1430m, 1375s, 1350m, 987s (CS); ^1H NMR (CDCl₃) δ 7.35–7.21 (m, 10H, Ph), 4.92 (s, 4H, CH₂Ph), 3.86 (s, 2H, H_{syn}), 2.70 (s, 2H, H_{anti}), 2.15 (s, 3H, Me); FAB MS (+ve) *m/z* 221 (15%), 377 (9%), 433 (3%), 595 (10%), 814 (2%). Anal. Calc. for Pd₁S₂N₁C₁₉H₂₁: C, 52.65; H, 4.84; N, 3.23. Found: C, 52.86; H, 4.73; N, 3.02%.

$[(\eta^3\text{-C}_4\text{H}_7)\text{Pd}(\text{S}_2\text{CNPr}_2)]$ (**1d**): red solid (69%); IR (KBr) 1525vs (CN), 1435m, 1375s, 1350m, 970s (CS); ^1H NMR (CDCl₃) δ 3.77 (s, 2H, H_{syn}), 3.67 (t, *J* 7.8, 4H, NCH₂), 2.62 (s, 2H, H_{anti}), 1.92 (s, 3H, Me), 1.73 (m, 4H, CH₂), 0.92 (t, *J* 7.8, 6H, Me); FAB MS (+ve) *m/z* 161 (21%),

250 (45%), 282 (97%), 337 (27%), 500 (52%), 621 (60%). Anal. Calc. for Pd₁S₂N₁C₁₁H₂₁: C, 39.17; H, 6.23; N, 4.15. Found: C, 39.54; H, 6.02; N, 4.02%. Single crystals suitable for diffraction studies were grown upon slow evaporation of a saturated diethyl ether solution.

$[(\eta^3\text{-C}_4\text{H}_7)\text{Pd}(\text{S}_2\text{CNBu}_2)]$ (**1e**): oily red solid (69%); ^1H NMR (CDCl₃) δ 3.77 (s, 2H, H_{syn}), 3.71 (t, *J* 7.3, 4H, NCH₂), 1.92 (s, 3H, Me), 1.66 (m, 4H, CH₂), 1.34 (sextet, *J* 7.5, 4H, CH₂), 0.90 (t, *J* 7.2, 6H, Me); FAB MS (+ve) *m/z* 312 (60%), 528 (91%), 677 (50%).

$[(\eta^3\text{-C}_4\text{H}_7)\text{Pd}(\text{S}_2\text{CNMeBu})]$ (**1f**): red oil (76%); ^1H NMR (CDCl₃) δ 3.77 (m, 4H, NCH₂ + H_{syn}), 3.30 (s, 3H, NMe), 2.62 (s, 2H, H_{anti}), 1.92 (s, 3H, Me), 1.64 (m, 2H, NCH₂CH₂), 1.34 (sex, *J* 7.6, 2H, NCH₂CH₂CH₂), 0.93 (t, *J* 7.3, 3H, Me); FAB MS (+ve) *m/z* 161 (20%), 236 (24%), 268 (94%), 323 (46%), 430 (5%), 486 (32%), 593 (25%).

$[(\eta^3\text{-C}_4\text{H}_7)\text{Pd}(\text{S}_2\text{CNMeHex})]$ (**1g**): red oil (82%); ^1H NMR (CDCl₃) δ 3.71 (m, 4H, NCH₂ + H_{syn}), 3.27 (s, 3H, NMe), 2.60 (s, 2H, H_{anti}), 2.08 (s, 3H, Me), 1.64 (m, 2H, NCH₂CH₂), 1.25 (m, 6H, CH₂), 0.82 (t, *J* 6.6, 3H, Me); FAB MS (+ve) *m/z* 264 (22%), 296 (100%), 351 (17%), 514 (40%), 617 (18%), 649 (41%), 720 (10%), 752 (18%), 784 (32%).

$[(\eta^3\text{-C}_4\text{H}_7)\text{Pd}(\text{S}_2\text{CNC}_5\text{H}_{10})]$ (**1h**): purple solid (74%); IR (KBr) 1490vs (CN), 1442m, 1401s, 1244m, 971s (CS); ^1H NMR (CDCl₃) δ 3.94 (m, 4H, NCH₂), 3.79 (s, 2H, H_{syn}), 2.63 (s, 2H, H_{anti}), 1.92 (s, 3H, Me), 1.67 (m, 6H, CH₂); FAB MS (+ve) *m/z* 266 (56%), 321 (45%), 426 (10%), 484 (56%), 557 (3%), 589 (25%). Anal. Calc. for Pd₁S₂N₁C₁₀H₁₇.0.5CH₂Cl₂: C, 34.56; H, 4.95; N, 3.85. Found: C, 36.25; H, 5.16; N, 3.73%.

$[(\eta^3\text{-C}_3\text{H}_5)\text{Pd}(\text{S}_2\text{CNMeBu})]$ (**2f**): brown solid (76%); IR (KBr) 1507vs (CN), 1437m, 1401s, 1299m, 962s (CS); ^1H NMR (CDCl₃) δ 5.09 (tt, *J* 12.6, 6.8, 1H, H_{central}), 3.98 (d, *J* 6.8, 1H, H_{syn}), 3.97 (d, *J* 6.8, 1H, H_{syn}), 3.74 (t, *J* 7.5, 2H, NCH₂), 3.28 (s, 3H, NMe), 2.73 (d, *J* 12.6, 2H, H_{anti}), 1.62 (m, 2H, NCH₂CH₂), 1.30 (sex, *J* 7.6, 2H, NCH₂CH₂CH₂), 0.90 (t, *J* 7.2, 3H, Me); FAB MS (+ve) *m/z* 236 (12%), 268 (31%), 309 (15%), 430 (8%), 579 (6%). Anal. Calc. for Pd₁S₂N₁C₉H₁₇.0.25CH₂Cl₂: C, 33.61; H, 5.30; N, 4.24. Found: C, 33.96; H, 5.21; N, 4.09%.

$[(\eta^3\text{-C}_3\text{H}_5)\text{Pd}(\text{S}_2\text{CNMeHex})]$ (**2g**): brown solid (78%); IR (KBr) 1517vs (CN), 1461m, 1398s, 1294m, 966s (CS); ^1H NMR (CDCl₃) δ 5.11 (tt, *J* 12.6, 6.9, 1H, H_{central}), 3.98 (d, *J* 6.9, 1H, H_{syn}), 3.97 (d, *J* 6.9, 1H, H_{syn}), 3.74 (m, 2H, NCH₂), 3.28 (s, 3H, NMe), 2.71 (d, *J* 12.6, 2H, H_{anti}), 1.66 (m, 2H, NCH₂CH₂), 1.28 (m, 6H, 3CH₂), 0.85 (t, *J* 6.8, 3H, Me); FAB MS (+ve) *m/z* 296 (15%), 486 (20%), 635 (4%), 750 (4%), 784 (15%). Anal. Calc. for Pd₁S₂N₁C₁₁H₂₁.0.5CH₂Cl₂: C, 36.36; H, 5.80; N, 3.69. Found: C, 37.24; H, 5.81; N, 3.68%.

$[(\eta^3\text{-C}_3\text{H}_5)\text{Pd}(\text{S}_2\text{CNC}_5\text{H}_{10})]$ (**2h**): purple solid (69%); IR (KBr) 1503vs (CN), 1439m, 1284m, 973s (CS); ^1H NMR (CDCl₃) δ 5.13 (tt, *J* 12.6, 7.0, 1H, H_{central}), 4.04 (d, *J* 7.0, 2H, H_{syn}), 3.96 (m, 4H, NCH₂), 2.74 (d, *J* 12.6, 2H, H_{anti}), 1.67 (m, 6H, CH₂); FAB MS (+ve) *m/z* 426 (33%),

575 (17%). Anal. Calc. for $\text{Pd}_1\text{S}_2\text{N}_1\text{C}_9\text{H}_{15}\cdot 0.5\text{CH}_2\text{Cl}_2$: C, 32.62; H, 4.58; N, 4.01. Found: C, 33.62; H, 4.53; N, 4.05%.

$[(\eta^3\text{-C}_6\text{H}_{11})\text{Pd}(\text{S}_2\text{CNMe}_2)]$ (**3a**): brown solid (80%); IR (KBr) 1520vs (CN), 1450m, 1395s, 1360m, 970s (CS); ^1H NMR (CDCl_3) δ 3.64 (br, 1H, H_{syn}), 3.35 (s, 6H, NMe), 2.94 (br, 1H, H_{anti}), 1.93 (s, 3H, Me), 1.67 (s, 3H, Me), 1.33 (s, 3H, Me); FAB MS (+ve) m/z 226 (18%), 311 (10%), 416 (25%), 500 (100%), 537 (13%). Anal. Calc. for $\text{Pd}_1\text{S}_2\text{N}_1\text{C}_9\text{H}_{17}$: C, 34.68; H, 5.78; N, 4.50. Found: C, 34.44; H, 5.70; N, 4.75%.

$[(\eta^3\text{-C}_6\text{H}_{11})\text{Pd}(\text{S}_2\text{CNEt}_2)]$ (**3b**): brown solid (82%); IR (KBr) 1505vs (CN), 1450m, 1425s, 1365m, 989s (CS); ^1H NMR (CDCl_3) δ 3.75–3.70 (m, 4H, NCH_2), 3.60 (s, 1H, H_{syn}), 2.84 (s, 2H, H_{anti}), 1.88 (s, 3H, Me), 1.64 (s, 3H, Me), 1.29 (s, 3H, Me), 1.20 (t, J 7.0, 6H, Me); FAB MS (+ve) m/z 154 (12%), 222 (33%), 254 (40%), 337 (21%), 402 (20%), 528 (100%). Anal. Calc. for $\text{Pd}_1\text{S}_2\text{N}_1\text{C}_9\text{H}_{17}$: C, 39.17; H, 6.23; N, 4.15. Found: C, 38.54; H, 6.21; N, 3.68%.

$[(\eta^3\text{-C}_6\text{H}_{11})\text{Pd}(\text{S}_2\text{CNBz}_2)]$ (**3c**): brown solid (60%); IR (KBr) 1500vs (CN), 1455m, 1375s, 1350m, 987s (CS); ^1H NMR (CDCl_3) δ 7.43–7.32 (m, 10H, Ph), 5.03–5.00 (br, 4H, CH_2Ph), 3.82 (s, 1H, H_{syn}), 3.08 (s, 1H, H_{anti}), 2.07 (s, 3H, Me), 1.84 (s, 3H, Me), 1.51 (s, 3H, Me); FAB MS (+ve) m/z 198 (100%), 346 (37%), 461 (8%), 652 (20%), 841 (43%). Anal. Calc. for $\text{Pd}_1\text{S}_2\text{N}_1\text{C}_{21}\text{H}_{25}$: C, 54.60; H, 5.42; N, 3.03. Found: C, 54.49; H, 5.40; N, 3.07%.

$[(\eta^3\text{-C}_6\text{H}_{11})\text{Pd}(\text{S}_2\text{CNPr}_2)]$ (**3d**): brown solid (74%); IR (KBr) 1500vs (CN), 1435m, 1375s, 1345m, 971s (CS); ^1H NMR (CDCl_3) δ 3.69 (q, J 6.0, 4H, NCH_2), 3.66 (s, 1H, H_{syn}), 2.92 (s, 1H, H_{anti}), 1.96 (s, 3H, Me), 1.74 (m, 4H, CH_2), 1.72 (s, 3H, Me), 1.37 (s, 3H, Me), 0.96 (t, J 7.8, 3H, Me), 0.92 (t, J 7.8, 3H, Me); FAB MS (+ve) m/z 144 (100%), 282 (46%), 365 (22%), 472 (10%), 556 (47%), 649 (43%). Anal. Calc. for $\text{Pd}_1\text{S}_2\text{N}_1\text{C}_{13}\text{H}_{25}$: C, 42.74; H, 6.85; N, 3.83. Found: C, 42.24; H, 6.69; N, 3.44%.

4.2. Synthesis of $[(\eta^3\text{-C}_4\text{H}_7)\text{Pd}(\text{S}_2\text{PPh}_2)]$ (**4**)

A methanol solution (10 cm^3) of NaS_2PPh_2 (0.136 g, 0.50 mmol) was added to a diethylether (40 cm^3) solution of $[(\eta^3\text{-C}_4\text{H}_7)\text{Pd}(\mu\text{-Cl})_2]$ (0.10 g, 0.25 mmol) in diethylether (40 cm^3). This was stirred for 1h resulting in the formation of a dark red precipitate. After filtration, washing with water ($2 \times 10 \text{ cm}^3$) and methanol (10 cm^3) gave a dark red solid which was air-dried to give $[(\eta^3\text{-C}_4\text{H}_7)\text{Pd}(\text{S}_2\text{PPh}_2)]$ (0.195 g, 95%). ^1H NMR (CDCl_3) δ 7.80 (br, 4H, Ph), 7.45 (br, 6H, Ph), 3.83 (s, 2H, H_{syn}), 2.75 (s, 2H, H_{anti}), 1.97 (s, 3H, Me); ^{31}P NMR (CDCl_3) δ 89.2 (s). Anal. Calc. for $\text{Pd}_1\text{S}_2\text{N}_1\text{C}_{16}\text{H}_{17}$: C, 46.78; H, 4.14. Found: C, 46.62; H, 4.29%. Single crystals suitable for diffraction studies were grown upon slow evaporation of a saturated diethyl ether solution.

4.3. Synthesis of $[\text{Pd}(\text{S}_2\text{CNMeBu})_2]$ (**5a**)

A methanol solution (10 cm^3) of $\text{NaS}_2\text{CNMeBu}$ (ca. 0.64 mmol) was prepared as described above. To this

was added $\text{Na}_2\text{PdCl}_4 \cdot 3\text{H}_2\text{O}$ (0.04 g, 0.32 mmol). A yellow precipitate immediately formed and this was stirred for 1 h. After filtration the solid was washed with water ($3 \times 10 \text{ cm}^3$) and methanol (10 cm^3) and air-dried to give $[\text{Pd}(\text{S}_2\text{CNMeBu})_2]$ (0.12 g, 87%) as a yellow-orange solid. ^1H NMR (CDCl_3) δ 3.68 (t, J 7.6, 4H, NCH_2), 3.24 (s, 6H, NMe), 1.63 (tt, J 9.2, 7.4, 4H, CH_2), 1.37 (sextet, J 7.4, 4H, CH_2), 0.95 (t, J 7.4, 6H, Me). Anal. Calc. for $\text{Pd}_1\text{S}_4\text{N}_2\text{C}_{12}\text{H}_{24}$: C, 33.45; H, 5.58; N, 6.50. Found: C, 34.14; H, 5.76; N, 6.44%. Single crystals suitable for diffraction studies were grown upon slow evaporation of a dichloromethane–diethyl ether solution.

4.4. $[\text{Pd}(\text{S}_2\text{CNMeHex})_2]$ (**5b**)

Prepared as above using HNMeHex to give a yellow-orange solid in 90% yield. ^1H NMR (CDCl_3) (328 K) δ 3.69 (brt, J 7.5, 4H, NCH_2), 3.25 (s, 6H, NMe), 1.69 (m, 4H, CH_2), 1.33 (br, 12H, CH_2), 0.90 (t, J 7.4, 6H, Me). Anal. Calc. for $\text{Pd}_1\text{S}_4\text{N}_2\text{C}_{16}\text{H}_{32}$: C, 39.47; H, 6.61; N, 5.78. Found: C, 39.33; H, 6.67; N, 5.57%.

4.5. PdS

Hydrogen sulfide was bubbled through an aqueous solution (20 cm^3) of Na_2PdCl_4 (1.00 g, 2.87 mmol) for 5 min. The solution was then stirred for a further 30 min resulting in the formation of a fine black precipitate. This was allowed to settle, collected by filtration and air-dried to give PdS as a black precipitate.

4.6. X-ray data collection and solution

Single crystals were mounted on glass fibres and all geometric and intensity data were taken from these samples using an automated four-circle diffractometer (Nicolet R3mV) equipped with Mo $\text{K}\alpha$ radiation ($\lambda = 0.71073 \text{ \AA}$) at $293 \pm 2 \text{ K}$. Lattice parameters were identified by application of the automatic indexing routine of the diffractometer to the positions of a number of reflections taken from a rotation photograph and centred by the diffractometer. The ω – 2θ (**1a**, **1c**, **4**) or ω techniques (**5a**) were used to measure reflections and three standard reflections (remeasured every 97 scans) showed no significant loss in intensity during data collections. The data were corrected for Lorentz and polarisation effects and unique data with $I \geq 2\sigma(I)$ were used to solve and refine the structures. These were solved by direct methods and developed by using alternating cycles of least-squares refinement and difference-Fourier synthesis. All non-hydrogen atoms were refined anisotropically. Hydrogen atoms were placed in idealised positions (C–H 0.96 \AA) and assigned a common isotropic thermal parameter ($U = 0.08 \text{ \AA}^2$). Final difference-Fourier map was featureless and contained no peaks greater than 1.00 e \AA^{-3} . Structure solution used SHELXTL PLUS program package on an IBM PC.

Crystallographic data for $[(\eta^3\text{-C}_4\text{H}_7)\text{Pd}(\text{S}_2\text{CNMe}_2)]$ (**1a**): orange needle, dimensions $0.45 \times 0.16 \times 0.06$ mm, monoclinic, space group $P2_1/m$, $a = 5.291(1)$ Å, $b = 10.576(2)$ Å, $c = 9.109(2)$ Å, $\beta = 92.83(3)^\circ$, $V = 509.1(2)$ Å³, $Z = 2$, $F(000) = 280$, $d_{\text{calc}} = 1.838$ g cm⁻³, $\mu = 2.173$ mm⁻¹. 1179 reflections were collected, 1057 unique [$R_{\text{int}} = 0.0347$] of which 977 were observed [$I > 2.0\sigma(I)$]. At convergence, $R_1 = 0.0387$, $wR_2 = 0.1013$ [$I > 2.0\sigma(I)$] and $R_1 = 0.0415$, $wR_2 = 0.1046$ (all data), for 61 parameters.

Crystallographic data for $[(\eta^3\text{-C}_4\text{H}_7)\text{Pd}(\text{S}_2\text{CNPr}_2)]$ (**1d**): pale yellow block, dimensions $0.80 \times 0.24 \times 0.22$ mm, triclinic, space group $P\bar{1}$, $a = 8.619(2)$ Å, $b = 9.373(2)$ Å, $c = 9.800(2)$ Å, $\alpha = 97.59(3)^\circ$, $\beta = 109.10(3)^\circ$, $\gamma = 89.86(3)^\circ$, $V = 740.9(3)$ Å³, $Z = 2$, $F(000) = 344$, $d_{\text{calc}} = 1.514$ g cm⁻³, $\mu = 1.507$ mm⁻¹. 2789 reflections were collected, 2599 unique [$R_{\text{int}} = 0.0244$] of which 2594 were observed [$I > 2.0\sigma(I)$]. At convergence, $R_1 = 0.0357$, $wR_2 = 0.0884$ [$I > 2.0\sigma(I)$] and $R_1 = 0.0408$, $wR_2 = 0.1044$ (all data), for 136 parameters.

Crystallographic data for $[(\eta^3\text{-C}_4\text{H}_7)\text{Pd}(\text{S}_2\text{PPh}_2)]$ (**4**): pale yellow plate, dimensions $0.46 \times 0.42 \times 0.06$ mm, monoclinic, space group $P2_1/c$, $a = 8.838(2)$ Å, $b = 12.494(2)$ Å, $c = 15.459(3)$ Å, $\beta = 94.60(3)^\circ$, $V = 1701.5(6)$ Å³, $Z = 4$, $F(000) = 824$, $d_{\text{calc}} = 1.604$ g cm⁻³, $\mu = 1.417$ mm⁻¹. 3151 reflections were collected, 2952 unique [$R_{\text{int}} = 0.0413$] of which 2943 were observed [$I > 2.0\sigma(I)$]. At convergence, $R_1 = 0.0486$, $wR_2 = 0.1111$ [$I > 2.0\sigma(I)$] and $R_1 = 0.0728$, $wR_2 = 0.5534$ (all data), for 181 parameters.

Crystallographic data for $[\text{Pd}(\text{S}_2\text{CNMeBu})_2]$ (**5a**): orange block, dimensions $0.43 \times 0.40 \times 0.27$ mm, hexagonal, space group $R\bar{3}$, $a = b = 25.654(4)$ Å, $c = 7.135(1)$ Å, $V = 4066.6(11)$ Å³, $Z = 9$, $F(000) = 1980$, $d_{\text{calc}} = 1.584$ g cm⁻³, $\mu = 1.478$ mm⁻¹. 925 reflections were collected, 917 unique [$R_{\text{int}} = 0.0136$] of which 908 were observed [$I > 2.0\sigma(I)$]. At convergence, $R_1 = 0.0317$, $wR_2 = 0.0720$ [$I > 2.0\sigma(I)$] and $R_1 = 0.0447$, $wR_2 = 0.0885$ (all data), for 88 parameters.

Acknowledgements

We thank AEA Technology for partial funding of this work and Mr. Mark Shilton for his interest, TUBITAK-BAYG for funding the visit of ES to UCL, Professor Ivan Parkin and Dr. Anne Newport for making powder X-ray measurements of the palladium sulfide sample, Dr. Marianne Odlyha for TGA and DSC measurements and Mr. Kevin Reeves for scanning electron microscopy.

Appendix A. Supplementary material

CCDC 628659, 628660, 628661 and 628662 contain the supplementary crystallographic data for this paper. These data can be obtained free of charge via <http://www.ccdc.cam.ac.uk/conts/retrieving.html>, or from the Cambridge

Crystallographic Data Centre, 12 Union Road, Cambridge CB2 1EZ, UK; fax: (+44) 1223-336-033; or e-mail: deposit@ccdc.cam.ac.uk. Supplementary data associated with this article can be found, in the online version, at doi:10.1016/j.jorganchem.2007.02.015.

References

- [1] A.A. Zirka, A.V. Mashkina, *Kinet. Catal.* 41 (2000) 888; A.A. Zirka, A.V. Mashkina, *Kinet. Catal.* 41 (2000) 521; A.V. Mashkina, L.G. Sakhaltueva, *Kinet. Catal.* 43 (2002) 107; A.V. Mashkina, L.N. Khairullina, *Kinet. Catal.* 43 (2002) 261; A. Ermakova, A.V. Mashkina, L.G. Sakhaltueva, *Kinet. Catal.* 43 (2002) 528; A. Daudin, S. Brunet, G. Perot, C. Bouchy, *Preprints – American Chemical Society, Division of Petroleum Chemistry*, vol. 51, 2006, p. 338.
- [2] T.M. Matveeva, N.V. Nekrasov, M.M. Kostyukovskii, M.D. Navalkhina, A.A. Krichko, S.L. Kiperman, *Bull. Acad. Sci. USSR Div. Chem. Sci.* 31 (1982) 1104; T.M. Matveeva, N.V. Nekrasov, M.M. Kostyukovskii, S.L. Kiperman, *Bull. Acad. Sci. USSR Div. Chem. Sci.* 33 (1984) 2227; L.V. Shalimova, A.D. Berents, S.V. Popov, O.V. Chebaeva, *Kinet. Catal.* 32 (1991) 45; N.D. Gavrilova, T.Y. Sergeeva, B.S. Gudkov, M.S. Kharson, S.L. Kiperman, *Kinet. Catal.* 32 (1991) 186.
- [3] N. Koizumi, A. Miyazawa, T. Furukawa, M. Yamada, *Chem. Lett.* (2001) 1282; N. Koizumi, K. Murai, S. Takasaki, M. Yamada, *Preprints of Symposia – American Chemical Society, Division of Fuel Chemistry* 46 (2001) 437.
- [4] A. Singhal, V.K. Jain, R. Mishra, B. Varghese, *J. Mater. Chem.* 10 (2000) 1121.
- [5] A.N. Gleizes, *Chem. Vapor Depos.* 6 (2000) 155.
- [6] J. Cheon, D.S. Talaga, J.I. Zink, *Chem. Mater.* 9 (1997) 1208.
- [7] M.A. Malik, P. O'Brien, N. Revaprasadu, *J. Mater. Chem.* 12 (2002) 92.
- [8] J. Powell, A.W.-L. Chan, *J. Organomet. Chem.* 35 (1972) 203.
- [9] R. Bertani, U. Belluco, P. Uguagliati, B. Crociani, *Inorg. Chim. Acta* 54 (1981) L279; B. Crociani, F. Di Bianca, M. Consiglio, M. Paci, P. Tagliatesta, *Inorg. Chim. Acta* 167 (1990) 171; B.E. Mann, P.M. Maitlis, *J. Chem. Soc., Chem. Commun.* (1976) 1058; S.H. Taylor, P.M. Maitlis, *J. Am. Chem. Soc.* 100 (1978) 4700; P.M. Bailey, S.H. Taylor, P.M. Maitlis, *J. Am. Chem. Soc.* 100 (1978) 4711; D.L. Reger, D.G. Garza, L. Lebioda, *Organometallics* 10 (1991) 902.
- [10] G. Hogarth, *Prog. Inorg. Chem.* 53 (2005) 71.
- [11] M. Mooriyasu, Y. Hashimoto, M. Endo, *Bull. Chem. Soc. Jpn.* 56 (1983) 1972.
- [12] F.F. Jian, F.L. Beia, P.S. Zhao, X. Wang, K.K. Fun, K. Chinnakali, *J. Coord. Chem.* 55 (2002) 429; M. Maekawa, M. Munakata, T. Kuroda-Sowa, M. Motokawa, *Anal. Sci.* 10 (1994) 977; L.Z. Xu, P.S. Zhao, S.S. Zhang, *Chin. J. Chem.* 19 (2001) 436.
- [13] M.-L. Riekkola, T. Pakkanen, L. Niinisto, *Acta Chem. Scand.* A 37 (1983) 807.
- [14] G.C. Franchini, A. Guisti, C. Preti, L. Jassi, P. Zannini, *Polyhedron* 4 (1985) 1553.
- [15] F. Grønvold, E. Røst, *Acta Chem. Scand.* 10 (1956) 1620.
- [16] Y. Zhang, R.J. Puddephatt, *Chem. Mater.* 11 (1999) 148.